A Microscopic Human-Inspired Adaptive Cruise Control for Eco-Driving

Marco Mirabilio, Alessio Iovine, Elena De Santis, Maria Domenica Di Benedetto, Giordano Pola

***Abstract*— In this paper a microscopic hybrid automaton for Adaptive Cruise Control (ACC) exhibiting psycho-physical human characteristics is introduced. The objective is to let the ACC mimic the human behavior to improve passenger experience, while assuring classical ACC properties. The human-inspired automaton in combined together with a predictive control strategy in order to meet physical and safety constraints, as well as the purpose of fuel minimization. Then, an optimization problem is formulated according to efficiency and constraints satisfaction and receding horizon techniques are used for its solution. Simulations are performed in order to validate the control law and to show the efficacy of the proposed approach.**

Keywords - Hybrid Automaton, Microscopic Models, Adaptive Cruise Control (ACC), Eco-driving, Model Predictive Control (MPC), fuel optimization.

I. INTRODUCTION

Adaptive Cruise Controls (ACCs) are nowadays becoming a reality thanks to the effort dedicated to their development in the last decades (see [1], [2], [3], [4]). The objective of ACCs is to offer human beings a safe and comfortable transportation with reduced congestion, emissions and travel time. Since the first works on ACCs, they took into account human factors such as comfort or safety perception in a control-oriented framework (see [5]), where the controllers were first designed according to some performance or stability-based criteria and secondly adapted to human characteristics by parameters' modifications. More recently there is a paradigm shift, and the main criteria for ad hoc control tool selection for ACCs is the correct human driving representation. Several works illustrates the usefulness of incorporating the driver's pose while designing ACCs in a control system framework (see [6], [7], [8], [1]), especially with respect to usually used rule-based models (see [9]).

The proposed work relies in this research line, and extends some previous results presented in [7], where a human-inspired hybrid automaton for ACC was proposed. It proposes a hybrid automaton modeling (see [10], [11]) to the purpose to solve an optimization problem for comfort maximization while emissions and fuel consumption minimization. The hybrid automaton capability to consider a number of control laws, one for each different situation, is exploited to let the ACC mimic the human driver behavior in a car-following situation. The discrete states of the hybrid automaton are used to capture the psycho-physical perception of the human while driving, such as the different feeling of risk felt in relation with the distance from other vehicles. The problem of computing the optimal speed, acceleration and fuel consumption (also referred to as eco-driving, as in [12], [13], [14], [15]) in a single-lane car-following scenario is addressed, in a Vehicle-to-Vehicle (V2V) communication framework.

We derive the consequent control laws taking into account human behavior imitation in the control loop (see [7]). A fuel-consumption/emission model based on vehicle speed and acceleration (see [16]) is considered for the implementation of a Model Predictive Control (MPC) strategy (see [17], [15]). The receding horizon technique is used to solve an optimal problem considering both safety and fuel consumption efficiency.

With respect to [7], where the considered control laws were developed by stimulus-response car-following models, here control strategies are derived by solving an optimization problem in order to maximize comfort and minimize emissions and fuel consumption. The structure of the hybrid automaton is simplified, but its human-inspired characteristics are preserved as the model is based on psycho-physical car-following models and stimulus-response ones are still considered in the definition of the cost functions. The developed control laws increase driving efficiency. Moreover, a more accurate dynamical model for the vehicle that includes dynamical friction is considered.

We consider N vehicles on a single lane road, sorted by location and indexed by $n \in \{1, ..., N\}$, where $n = 1$ denotes the first vehicle on the lane. Then, for each leader and follower pair $(n, n+1)$, $n = 1, ..., N-1$, a simplified hybrid automaton is developed, based on psycho-physical car-following models. Therefore the modeling of the traffic flow is microscopic. Here, control strategies are derived by solving an optimization problem in order to maximize comfort and minimize emissions and fuel consumption. Moreover, a more accurate dynamical model for the vehicle that includes dynamical friction is considered. Simulations show the validity of the adopted model and the simulation results are illustrated.

The paper is organized as follows. Section II introduces the problem. In Section III the model of the microscopic hybrid automaton for a single vehicle is described. Then in Section IV the proposed control technique is illustrated. Section V provides simulation results about the system behaviour. Finally, conclusions are offered in Section VI.

The research leading to these results has received funding from the Italian Government under Cipe resolution n.135 (Dec. 21, 2012), project INnovating City Planning through Information and Communication Technologies (INCIPICT).

Department of Information Engineering, Computer Science and Mathematics, Center of Excellence DEWS, University of LAquila. (e-mail:marco.mirabilio@graduate.univaq.it,alessio.iovine@ieee.org, {elena.desantis,mariadomenica.dibenedetto,giordano.pola}@univaq.it)

II. Problem definition

We suppose that the single vehicle can be described by a triple integrator, discretized with sampling time τ, where the control input is the acceleration variation (jerk). Moreover, friction is taken into account by adding a nonlinear term. If $k\tau,\ k \in \mathbb{N}$ denotes the k-th sampling time, then the variables describing the evolution of vehicle $n,\ n = 1, ..., N$, are the longitudinal position ($p^n(k) \geq 0, [m]$), velocity ($0 \leq v^n(k) \leq v_{\max}, [m/s]$) and acceleration ($|a^n(k)| \leq a_{\max}, [m/s^2]$).

Let the pair $(n, n+1),\ n = 1, ..., N-1$, denote leader vehicle (n) and follower vehicle ($n+1$). Then the follower's state vector is defined as

$$x^{n+1}(k) = \begin{bmatrix} x_1^{n+1}(k) \\ x_2^{n+1}(k) \\ x_3^{n+1}(k) \\ x_4^{n+1}(k) \end{bmatrix} = \begin{bmatrix} p^n(k) - p^{n+1}(k) \\ v^n(k) - v^{n+1}(k) \\ a^{n+1}(k) \\ v^n(k) \end{bmatrix} \quad (1)$$

In the following we omit the index $n+1$, for notational simplicity. For the first vehicle of the cluster we assume that there exists a virtual leader $n = 0$, such that $v^0(k) = v_{\max}$ and $a^0(k) = 0\ \forall k \in \mathbb{N}$. Physical and legal limits lead to the following constraint set $X \subseteq \mathbb{R}^4$ of feasible states for $x(k)$:

$$X = \left\{x \in \mathbb{R}^4 : x_1 \geq s, |x_2| \leq v_{\max}, |x_3| \leq a_{\max}, 0 \leq x_4 \leq v_{\max}\right\} \quad (2)$$

where s is related to the definition of collision:

Definition 1: A *collision* is the event corresponding to a distance between two vehicles less than $s = L + L_0,\ L_0 \in \mathbb{R}^+$.

The discrete-time evolution of the continuous state is described by

$$x(k+1) = Ax(k) + B_u u(k) + B_d d(k) + Ee(x(k)) \quad (3)$$

where

$$A = \begin{bmatrix} 1 & \tau & 0 & 0 \\ 0 & 1 & -\tau & 0 \\ 0 & 0 & 1 & 0 \\ 0 & 0 & 0 & 1 \end{bmatrix}, B_u = \begin{bmatrix} 0 \\ 0 \\ \tau \\ 0 \end{bmatrix}, B_d = \begin{bmatrix} 0 \\ \tau \\ 0 \\ \tau \end{bmatrix}, E = \begin{bmatrix} 0 \\ \tau \\ 0 \\ 0 \end{bmatrix}$$

$|u(k)| \leq u_{\max}$ is the jerk of vehicle $n+1$; $e(x) = c_1 + c_2(x_4 - x_2)^2,\ c_1, c_2 > 0$, is a nonlinear term representing friction (see [18]); $d(k) = a^n(k)$ is the acceleration, modeled as a bounded disturbance $|d(k)| \leq a_{\max}$, of the vehicle ahead n.

We make the following

Assumption 1: All vehicles in the cluster share the goal of avoiding collisions. To this purpose we assume that the follower knows position and velocity of its predecessor.

The follower can obtain information about its leader either by inter-vehicle communications (implementing the so called Cooperative ACC) or by the use of sensors installed on the vehicle, in order to be able to estimate the cited variables (see [7]). The leader's acceleration, velocity and position are assumed to be known.

Given the dynamic model of the vehicle, the problem we want to solve is to find a set of initial states contained in X such that the state trajectory of the controlled system always lies in X (safety specification). Among all the control laws that ensure safety, we compute the optimal one that minimizes a state-dependent cost function, which takes into account emissions (eco-driving specifications) and errors with respect to a desired distance between two consecutive vehicles and a desired velocity. Since we are interested in taking into account human safety and comfort perception, the set X is partitioned on the basis of *psycho-physical thresholds* in order to separate the different psychological situations the driver feels (see [19], [20], [7]). To each set of the partition, different cost function parameters are associated. For this reason, because of the possibility of describing various dynamics in a unique model, hybrid systems theory (see [11]) is used and a hybrid automaton is defined that collects all the different behaviours.

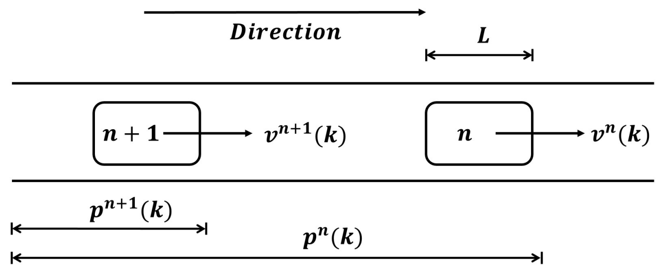

Fig. 1. The reference framework.

III. Microscopic Hybrid Model

In this section, a microscopic hybrid model that describes a car-following situation is presented, which simplifies the one proposed in [7]. Given a pair $(n, n+1)$ of vehicles, the hybrid automaton describing the follower is

$$\mathcal{H} = (Q, \mathbb{R}^4, U, D, f, Init, Dom, \mathcal{E}) \quad (4)$$

where: $Q = \{q_i,\ i = 1, 2, 3, 4\}$ is the set of discrete states; $\mathbb{R}^4$ is the continuous state space; $U = \mathbb{R}$ is the input space; $D = \mathbb{R}$ is the disturbance space; $f = \{f_i,\ q_i \in Q\}$, $f_i : \mathbb{R}^4 \times U \times D \to \mathbb{R}^4$ is a vector field that associates to the discrete state $q_i \in Q$ the discrete time-invariant dynamics

$$x(k+1) = f_i(x(k), u(k), d(k)),\ k \in \mathbb{N} \quad (5)$$

with $u : \mathbb{N} \to U$ and $d : \mathbb{N} \to D$; $Init \subseteq Q \times \mathbb{R}^4$ is the set of initial discrete and continuous conditions; $Dom : Q \to 2^{\mathbb{R}^4}$ is the domain map; $\mathcal{E} \subseteq Q \times Q$ is the set of edges.

The automaton hybrid state is the pair $(x, q_i) \in \mathbb{R}^4 \times Q$. As we will see later in the paper, the domains of each discrete state are such that $Dom(q_i) \cap Dom(q_j) = \emptyset, i \neq j$. Moreover, the continuous dynamics (3) is associated to each discrete state.

We define the functions $T_E : \mathbb{R}^4 \to \mathbb{R}$, $T_R : \mathbb{R}^4 \to \mathbb{R}$ and $T_S : \mathbb{R}^4 \to \mathbb{R}$, as

$$T_E(x) = \frac{|x_2|}{a_{\max}},\ T_R(x) = \frac{|x_4 - x_2|}{a_{\max}},\ T_S(x) = \lambda \frac{|x_4 - x_2|}{a_{\max}}, \quad (6)$$

that represent, respectively, the time headways needed to stop the vehicle from speed x_2 and $|x_4 - x_2|$ with deceleration $x_3(k) = -a_{\max}$ and the time needed to stop the vehicle from speed $|x_4 - x_2|$ with $x_3(k) = -\frac{a_{\max}}{\lambda}$, $\lambda > 1$. On the basis of these time headways, we define the thresholds for the space headway $x_1(k)$, which reflect the human driver perception:

- *emergency distance* $\Delta E : \mathbb{R}^4 \rightarrow \mathbb{R}$

$$\Delta E(x) = \begin{cases} s & x_2 > 0 \\ s + \frac{1}{2} a_{\max} T_E^2(x) & x_2 \leq 0 \end{cases} \tag{7}$$

  represents the minimum distance where safety is ensured (see [21]). If at time k the headway is equal to $\Delta E(x(k))$ and the leader brakes with the maximum deceleration, provided that the follower also brakes at the same time with the maximum deceleration, then collision is avoided. Due to the fact we are in a discrete time setting and the controller acts on the acceleration variation, we have to take into account a delay in the action of the control in the two first state components. Then, we define the additional safety distance that depends on the sampling time τ:

$$\Delta E'(x) = \begin{cases} s + 0.5 a_{\max} \tau^2, & x_2 > 0. \\ s + 0.5 a_{\max} (T_E(x) + \tau)^2, & x_2 \leq 0. \end{cases} \tag{8}$$

  It follows that the continuous model is a limit case with $\tau = 0$, in which $\Delta E(x) = \Delta E'(X)$.
- *risky distance* $\Delta R : \mathbb{R}^4 \rightarrow \mathbb{R}$

$$\Delta R(x) = \begin{cases} s + c_r T_R(x) x_4 & x_2 > 0 \\ s + c_r T_R(x) x_4 + \frac{1}{2} a_{\max} T_E^2(x) & x_2 \leq 0 \end{cases} \tag{9}$$

  has the same interpretation as the distance $\Delta E(x)$, but it takes into account a human time-response, modeled by the add-on value $c_r T_R(x) x_4$, where $c_r > 0$ is a constant multiplication factor. Depending on the environment information and on the human perception, such value can increase (more caution behaviour), or decrease (more aggressive behaviour), but the condition $\Delta R(x) > \Delta E(x)$ is always satisfied.
- *safe distance* $\Delta S : \mathbb{R}^4 \rightarrow \mathbb{R}$

$$\Delta S(x) = \begin{cases} s + c_s T_S(x) x_4 & x_2 > 0 \\ s + c_s T_S(x) x_4 + \frac{1}{2} a_{\max} T_E^2(x) & x_2 \leq 0 \end{cases} \tag{10}$$

  corresponds to an additional safety margin w.r.t. $\Delta R(x)$; in fact $c_s \geq c_r$ and $\lambda > 1$ imply that $T_S > T_R$ and hence $\Delta S(x) > \Delta R(x)$.
- *interaction distance* $\Delta D : \mathbb{R}^4 \rightarrow \mathbb{R}$

$$\Delta D(x) = \begin{cases} s + c_s T_S(x) x_4 & x_2 > 0 \\ s + T_D(x_4 - x_2) & x_2 \leq 0 \end{cases} \tag{11}$$

  where T_D is a fixed time: it is the time headway beyond which the vehicle can take the role of a leader (see [19], [20]).
  Note that when $x_2 > 0$, i.e. when $v^n(t) > v^{n+1}(t)$, $\Delta D(x) = \Delta S(x)$.

Similarly to [7], these space thresholds are used to define the partition of the state space $\mathbb{R}^4$ to be associated to each discrete state q_i, as follows.

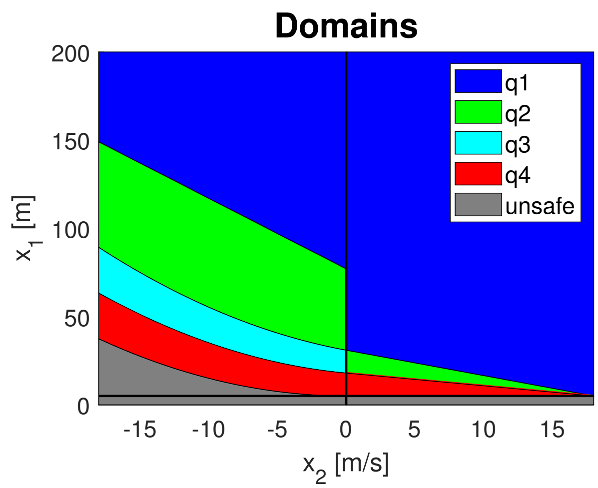

Fig. 2. The different thresholds and the corresponding domains at a fixed $\mathbf{v}^n = 18$ m/s: q_1 domain is blue, q_2 green, q_3 cyan and q_4 red. The unsafe region is in grey. Here $\tau = 0$ is considered.

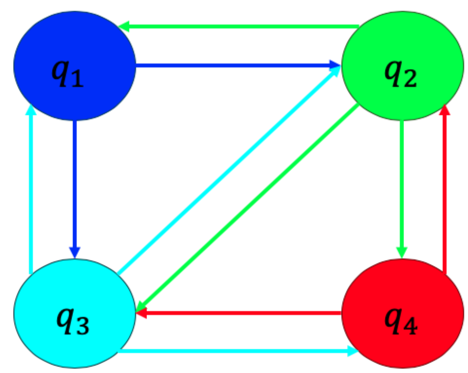

Fig. 3. The discrete states considered and their transitions. Colors are related to the domains depicted in Fig. 2.

1) q_1: Free driving. $Dom(q_1)$ is the set

$$\begin{aligned} &\left\{x \in \mathbb{R}^4 : (x_1 > \mathbf{l}_A) \wedge (x_2 \geq 0)\right\} \\ &\cup \left\{x \in \mathbb{R}^4 : (x_1 > \mathbf{l}_B) \wedge (x_2 < 0)\right\} \end{aligned} \tag{12}$$

   where $\mathbf{l}_A = \max\{\Delta S(x), \Delta E'(x)\}$, $\mathbf{l}_B = \max\{\Delta D(x), \Delta S(x), \Delta E'(x)\}$. The vehicle is expected to positively accelerate since the leader vehicle is either too far away or faster or both and the current speed is less than the desired one: $0 \leq x_3 \leq a_{\max}$. v_{des} is the desired speed to achieve; we assume that $v_{des} = \mathbf{v}_{\max}$. The control action will depend on the desired speed and on the fuel consumption rate.

2) q_2: Following I. $Dom(q_2)$ is the set

$$\begin{aligned} &\left\{x \in \mathbb{R}^4 : (\mathbf{m}_A < x_1 \leq \mathbf{l}_A) \wedge (x_2 \geq 0)\right\} \\ &\cup \left\{x \in \mathbb{R}^4 : (\mathbf{m}_B < x_1 \leq \mathbf{l}_B) \wedge (x_2 < 0)\right\} \end{aligned} \tag{13}$$

   where $\mathbf{m}_A = \max\{\Delta R(x), \Delta E'(x)\}$ and $\mathbf{m}_B = \max\{\Delta E'(x), \min\{\Delta D(x), \Delta S(x)\}\}$. Here the follower is closing in on the leader. The control action will depend on the fuel consumption, relative speed and distance.

3) q_3: Following II. $Dom(q_3)$ is the set

$$\begin{aligned}&\{x \in \mathbb{R}^4 : (x_1 = \mathbf{m}_A) \wedge (x_2 = 0)\} \cup \\ &\{x \in \mathbb{R}^4 : (\mathbf{m}_A < x_1 \le \mathbf{m}_B \wedge (x_2 < 0)\}\end{aligned} \tag{14}$$

The speed difference is large and the distance is not, so the follower has to decelerate depending on distance and relative speed. The control action depends on relative speed, distance and fuel consumption.

4) q_4: Closing in. $Dom(q_4)$ is the set

$$\begin{aligned}&\{x \in \mathbb{R}^4 : (\Delta E'(x) \le x_1 \le \Delta R(x))\} \setminus \\ &\{x \in \mathbb{R}^4 : (x_2 = 0) \wedge (x_1 = \mathbf{m}_A)\}\end{aligned} \tag{15}$$

The distance from the previous vehicle is close to the unsafe one: the control action depends only on relative speed and distance.

The $Init$ set can be defined as

$$Init = \bigcup_{i=1}^{4} (\{q_i\} \times (Dom(q_i) \cap X)) \tag{16}$$

Figure 2 shows the domains obtained by setting $v^n = \mathbf{v}^n$ constant and $\tau = 0$. The results are represented in a bi-dimensional space: the speed difference ($x_2(k)$) and the distance ($x_1(k)$) are reported on the abscissa and ordinate respectively. Figure 3 shows the admissible transitions between the discrete states.

Recall that a set $\Psi \subset \mathbb{R}^4$ is robustly controlled invariant for system (3) if for any $x \in \Psi$ there exists $u \in \mathbb{R}$ such that $Ax + B_u u + B_d d + Ee(x) \in \Psi$, $\forall d \in \mathbb{R}$, $|d| \le a_{\max}$.

We define $\Omega = \left(\bigcup_{i=1}^{4} Dom(q_i) \cap X\right)$. Since Ω is a convex set, the following holds:

Proposition 1: The set Ω is robustly controlled invariant for system (3).

Proof: The set Ω is by construction controlled invariant for system (3), with $e(x(k)) = 0, \forall k$. In fact it is straightforward to verify that the control law $u(x(k)) = -x_3(k) - a_{\max}$ makes Ω invariant. Since $e(x(k))$ is positive $\forall k$, its effect is to increase the second component of the state, and hence it reduces the follower velocity. Therefore the set Ω is robustly controlled invariant for system (3). ■

Proposition 1 shows that the domains we have defined make it possible to control the system in such a way that safety is ensured in the worst case scenario, i.e. the situation where the deceleration of one or more vehicles in the cluster is maximum. The grey region in Fig. 2 represents the unsafe region. Since there exists a control law such that this region is never reached starting from Ω, for simplicity we have not defined the unsafe discrete state, with that grey region as domain.

Proposition 2: The hybrid automaton $\mathcal{H}$ controlled by any control law that makes the set Ω robustly invariant, is non-blocking and deterministic.

Proof: Given a control law which makes the set Ω robustly invariant, the hybrid state evolution remains in $Init$ whenever the initial state belongs to $Init$. Therefore the controlled automaton is non-blocking. Determinism comes by definition, because the intersection between any two different domains is empty. ■

IV. Control Design

The purpose of this section is to find an optimal solution to the safety and fuel consumption problem, according to the different situations the driver is exposed to. These situations are represented by the hybrid automaton discrete states, for which we define different objectives trading-off between fuel optimization and pure safety.

To reduce computational effort, some simplifications are made. For every $q_j \in Q$ a fixed prediction horizon $\mathcal{N}_j \in \mathbb{N}$ is given, and a cost function J_j is chosen so that the various objectives receive different weights, as a human driver would do. We make a prediction of the leader acceleration in the near future, based on the current information. This results in a disturbance vector to be used in the MPC algorithm

$$\mathbf{d} = [a^n(k), \bar{a}^n(k+1), ..., \bar{a}^n(k+\mathcal{N}_j)]^T \tag{17}$$

where $\bar{a}^n(k+i) = a^n(k)$ until the corresponding predicted leader velocity $\bar{v}^n(k+i) \in [0, v_{\max}]$, otherwise $\bar{a}^n(k+i) = 0$; $i = 1, ..., \mathcal{N}_j$ is the generic time instant. Note that recently (see [18]) the possibility that the leader vehicle itself communicating its own acceleration prediction was introduced. At each time k, the control law $u(k)$ is calculated according to the current discrete state q_j and consequently to a unique dedicated cost function J_j. Then, a new measurement of the current state $x(k+1)$ is taken at time $k+1$, and the proper control law $u(k+1)$ is computed according to the current discrete state q_i, that may be equal or different from the previous q_j. This leads to a suboptimal solution of the general problem, since no prediction of the future discrete state is computed, but has the advantage of avoiding to solve a NP-hard problem (see [22]). Under the assumption that the entire state is measurable, the vector y is defined as

$$\begin{aligned}&y_i = x_i \text{ for } i = 1, 2, 3 \\ &y_4 = x_4 - x_2\end{aligned} \tag{18}$$

and the output reference vector y^r as

$$y^r = \begin{bmatrix} \Delta S_{des} & 0 & 0 & v_{des} \end{bmatrix}^T \tag{19}$$

where ΔS_{des} and v_{des} denote, respectively, the desired distance and velocity, assumed to be constant in the prediction window. Then, the error between y and y^r is $\tilde{y} = y - y^r$.

Given the current hybrid state at time k

$$(\bar{x}, q_j), \ \bar{x} \in Dom(q_j) \tag{20}$$

the problem is to find

$$\min_{u(h),\ h=0,\dots,\mathcal{N}_j-1} J_j \tag{21}$$

where

$$\begin{aligned}J_j = \frac{1}{2}\left[\tilde{y}^T(\mathcal{N}_j)P_j\tilde{y}(\mathcal{N}_j) + M_j \sum_{h=0}^{\mathcal{N}_j} \exp\left(w^T(h)P_j^C z(h)\right)\right] + \\ + \frac{1}{2}\left[\sum_{h=0}^{\mathcal{N}_j-1}\left(\tilde{y}^T(h)G_j\tilde{y}(h) + u^T(h)R_j u(h)\right)\right]\end{aligned} \tag{22}$$

subject to

$$x(h+1) = Ax(h) + B_u u(h) + B_d \mathbf{d}(h) + Ee(x(h)), \forall\, h \in \mathbb{N},$$
$$x(0) = \bar{x},$$
$$x(h) \in \Omega, \forall\, h \in \mathbb{N}$$

where

$$z^T = \begin{bmatrix} 1 & y_3 & y_3^2 & y_3^3 \end{bmatrix}, \quad w^T = \begin{bmatrix} 1 & y_4 & y_4^2 & y_4^3 \end{bmatrix}. \tag{23}$$

are the operators introduced in [17] that are related to the estimation of CO, NO_x and HC emissions. The term $\exp\left(w^T(h) P_j^C z(h)\right)$ represents the instantaneous fuel consumption or emission rate ($[l/s]$ or $[mg/s]$), where matrix P_j^C is differently defined for positive ($P_j^C = P_j^{C+}$) and negative accelerations ($P_j^C = P_j^{C-}$), as described in (see [16] and [15]). Which of the two forms of P_j^C is used in the cost function is determined in a heuristic way, assuming that according to the current discrete state it is reasonable to suppose that the vehicle will accelerate (as in q_2) or decelerate (as in q_3) in the immediate future. Matrices P_j and G_j are semidefinite positive and $R_j, M_j \geq 0$.

By Proposition 1, since Ω is robustly controlled invariant, problem (21) is feasible for any $(\bar{x}, q_j) \in Init$. Let $u^*(h),\ h = 0, ..., \mathcal{N}_j - 1$, be the optimal solution to problem (21), then the control input at time k is $u(k) = u^*(0)$.

A more detailed description of the different cost functions associated to the discrete states $q_j \in Q$ follows:

1) $j = 1$. The leader vehicle is either too far away or faster or both; then the follower is free to track the desired speed v_{des}, without incurring immediate dangers, applying fuel consumption optimization with respect to a desired speed. We set $p_{44} > 0$ and $g_{44} > 0$ (other elements of P_1 and G_1 are null), $R_1 > 0$, $M_1 > 0$. $P_j^C = P_j^{C+}$ because the vehicle is expected to be at lower velocity, or at most at the same one.
2) $j = 2$. The follower is closing in to the leader, but distance and velocity are such that there is no immediate danger. The proposed cost function allows for an optimal tracking of the desired distance ΔS_{des} considering both relative distance error and fuel consumption. We set $p_{11} > 0$, $p_{22} > 0$, $g_{11} > 0$, $g_{22} > 0$ (other elements of P_2 and G_2 are null), $R_2 > 0$, $M_2 > 0$ and $P_j^C = P_j^{C+}$.
3) $j = 3$. The speed difference is large and the distance is not, so the vehicle has to decelerate depending on distance and relative speed. The proposed cost function allows for an optimal tracking of the desired distance ΔS_{des} considering both the relative distance error and fuel consumption. We set $p_{11} > 0$, $p_{22} > 0$, $g_{11} > 0$, $g_{22} > 0$ (other elements of P_3 and G_3 are null), $R_3 > 0$, $M_3 > 0$ and $P_j^C = P_j^{C-}$.
4) $j = 4$. The distance from the previous vehicle is close to the unsafe one. The proposed cost function allows for an optimal tracking of the desired distance ΔS considering only relative distance error, since safety has priority over fuel optimization. We set $p_{11} > 0$, $p_{22} > 0$, $g_{11} > 0$, $g_{22} > 0$ (other elements of P_4 and G_4 are null), $R_4 = 0$, $M_4 = 0$ and $P_j^C = P_j^{C-}$.

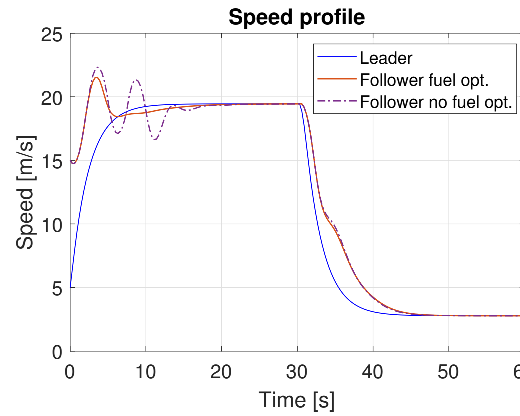

Fig. 4. The speed profile of the leader (blue line) and of the follower in the first (fuel opt., red line) and second case (no fuel opt., dotted line).

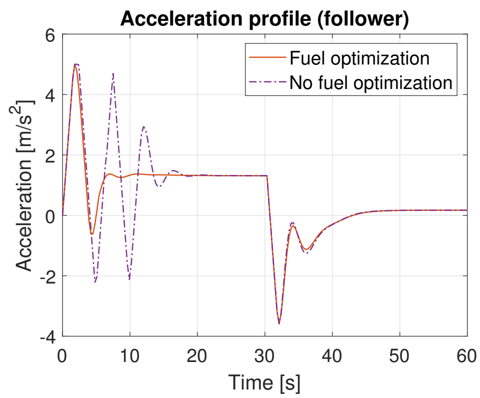

Fig. 5. The acceleration profile of the follower in the first (fuel opt., red line) and second case (no fuel opt., dotted line).

V. Simulations

In this section, simulation results obtained by using Matlab-Simulink and the optimization toolbox Yalmip (see [23]) are illustrated.

A car-following situation among two vehicles is considered and two cases are shown: in the first case fuel optimization is considered (i.e. $M_j \neq 0$), while in the second case fuel consumption is not taken into account ($M_j = 0, \forall j \in \{1,2,3,4\}$). Both cases consider the same initial conditions ($x_1(0) = 60$, $x_2(0) = -10$, $x_3(0) = 0$, $x_4(0) = 5$, $u(0) = 0$) and the same velocity profile of the leader: the leader first accelerates from 5m/s to reach the desired speed of 18m/s, and then decelerates (Fig. 4). The considered prediction horizon is $\mathcal{N}_j = 10, \forall j$, and the desired distance is $\Delta S_{des} = \Delta S(x(k))$ (see (10)). For the follower, this corresponds to track a safe distance that varies in relation with the current speed. As shown in Fig. 7, the proposed control laws indeed ensure collision-free car-following behavior. In Fig. 5 acceleration profiles associated with the two different control laws are shown: we can see how the solution corresponding to fuel optimization

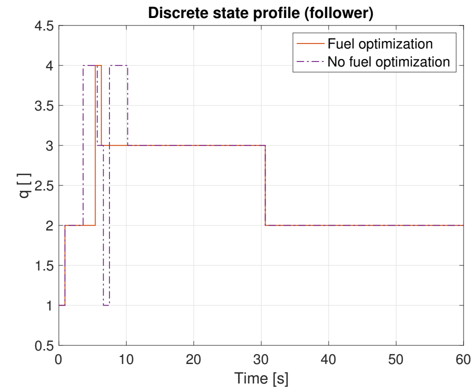

Fig. 6. The discrete state evolution of the follower in the first (fuel opt., red line) and second case (no fuel opt., dotted line).

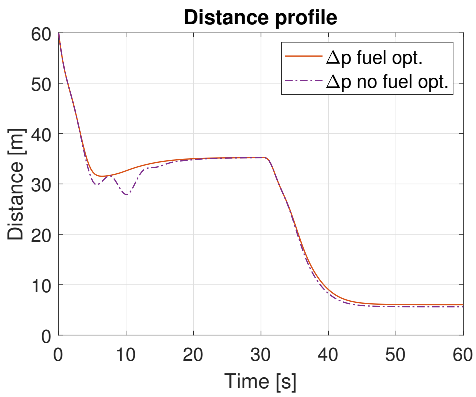

Fig. 7. Intervehicular distances in the first (fuel opt., red line) and second case (no fuel opt., dotted line).

(first case) is smoother, allowing the vehicle to produce less dangerous emissions, but also to reduce possible negative oscillations in the platoon. This acceleration profile has also impact on the speed profile (Fig. 4), presenting a similar smoother behavior: when comparing acceleration profiles of the two cases (Fig. 5), fuel optimization allows for a shorter transient (around 4s instead of 20s), and it also produces dynamics with less oscillations. Note that less transitions in the discrete evolution are obtained with fuel optimization (Fig. 6). The small improvement which is obtained in the first overshoot is also confirmed in the deceleration phase after 30s (see Fig. 5). In Fig.7 the distance profile evolution between leader and follower is shown. It can be seen that in the case of fuel optimization, the follower remains at a greater distance; then collision avoidance is enforced. Further extensions to a more complex scenario, possibly containing several driving cycles, will be investigated in future works.

VI. Conclusions

A human-inspired ACC for eco-driving for autonomous vehicles is proposed, focusing on the possibility of implementing predictive control strategies to maximize the human idea of comfort given by some psychological thresholds and minimize the fuel consumption. A dedicated hybrid automaton is presented, and some key properties are verified. Simulation results show the effectiveness of the proposed control strategy in obtaining a safe collision-free car-following situation together with fuel consumption minimization. Future work will extend the proposed approach by including macroscopic quantities.

References

[1] J. Guanetti, Y. Kim, and F. Borrelli, "Control of connected and automated vehicles: State of the art and future challenges," *Annual Reviews in Control*, vol. 45, pp. 18 – 40, 2018.

[2] K. Bengler, K. Dietmayer, B. Farber, M. Maurer, C. Stiller, and H. Winner, "Three Decades of Driver Assistance Systems: Review and Future Perspectives," *IEEE Intelligent Transportation Systems Magazine*, vol. 6, no. 4, pp. 6–22, winter 2014.

[3] P. Ioannou and C. Chien, "Autonomous intelligent cruise control," *Vehicular Technology, IEEE Transactions on*, vol. 42, no. 4, pp. 657–672, Nov 1993.

[4] P. Varaiya, "Smart cars on smart roads: problems of control," *Automatic Control, IEEE Transactions on*, vol. 38, no. 2, pp. 195–207, Feb 1993.

[5] M. Elbanhawi, M. Simic, and R. Jazar, "In the Passenger Seat: Investigating Ride Comfort Measures in Autonomous Cars," *IEEE Intelligent Transportation Systems Magazine*, vol. 7, no. 3, pp. 4–17, 2015.

[6] V. Shia, Y. Gao, R. Vasudevan, K. Campbell, T. Lin, F. Borrelli, and R. Bajcsy, "Semiautonomous vehicular control using driver modeling," *Intelligent Transportation Systems, IEEE Transactions on*, vol. 15, no. 6, pp. 2696–2709, Dec 2014.

[7] A. Iovine, F. Valentini, E. De Santis, M. Di Benedetto, and M. Pratesi, "Safe human-inspired mesoscopic hybrid automaton for autonomous vehicles," *Nonlinear Analysis: Hybrid Systems*, vol. 25, pp. 192 – 210, 2017.

[8] C. Lv, X. Hu, A. Sangiovanni-Vincentelli, Y. Li, C. M. Martinez, and D. Cao, "Driving-style-based codesign optimization of an automated electric vehicle: A cyber-physical system approach," *IEEE Transactions on Industrial Electronics*, vol. 66, no. 4, pp. 2965–2975, 2019.

[9] A. Kesting, M. Treiber, M. Schnhof, and D. Helbing, "Adaptive cruise control design for active congestion avoidance," *Transportation Research Part C: Emerging Technologies*, vol. 16, no. 6, pp. 668 – 683, 2008.

[10] P. Nilsson, O. Hussien, A. Balkan, Y. Chen, A. D. Ames, J. W. Grizzle, N. Ozay, H. Peng, and P. Tabuada, "Correct-by-construction adaptive cruise control: Two approaches," *IEEE Transactions on Control Systems Technology*, vol. 24, no. 4, pp. 1294–1307, 2016.

[11] J. Lygeros, K. H. Johansson, S. N. Simic, J. Zhang, and S. S. Sastry, "Dynamical properties of hybrid automata," *IEEE Transactions on Automatic Control*, vol. 48, no. 1, pp. 2–17, Jan 2003.

[12] A. Sciarretta, G. De Nunzio, and L. L. Ojeda, "Optimal ecodriving control: Energy-efficient driving of road vehicles as an optimal control problem," *IEEE Control Systems*, vol. 35, no. 5, pp. 71–90, 2015.

[13] J. Han, A. Vahidi, and A. Sciarretta, "Fundamentals of energy efficient driving for combustion engine and electric vehicles: An optimal control perspective," *Automatica*, vol. 103, pp. 558 – 572, 2019.

[14] M. A. S. Kamal, M. Mukai, J. Murata, and T. Kawabe, "Model predictive control of vehicles on urban roads for improved fuel economy," *IEEE Transactions on Control Systems Technology*, vol. 21, no. 3, pp. 831–841, 2013.

[15] S. Lin, B. De Schutter, Y. Xi, and H. Hellendoorn, "Integrated urban traffic control for the reduction of travel delays and emissions," *IEEE Transactions on Intelligent Transportation Systems*, vol. 14, no. 4, pp. 1609–1619, 2013.

[16] K. Ahn, H. Rakha, A. Trani, and M. Van Aerde, "Estimating vehicle fuel consumption and emissions based on instantaneous speed and acceleration levels," *Journal of transportation engineering*, vol. 128, no. 2, pp. 182–190, 2002.

[17] S. K. Zegeye, B. D. Schutter, H. Hellendoorn, and E. Breunesse, "Reduction of travel times and traffic emissions using model predictive control," in *2009 American Control Conference*, 2009, pp. 5392–5397.

[18] V. Turri, Y. Kim, J. Guanetti, K. H. Johansson, and F. Borrelli, "A model predictive controller for non-cooperative eco-platooning," in *2017 American Control Conference*, May 2017, pp. 2309–2314.

[19] R. U. Wiedemann, R., "Microscopic traffic simulation: the simulation system mission," 1991.

[20] H. Fritzsche, "A model for traffic simulation," *Traffic Engineering and Control*, vol. 35, no. 5, pp. 317–321, May 1994.
[21] P. Gipps, "A behavioural car-following model for computer simulation," *Transportation Research B*, 1981.
[22] A. Bemporad and M. Morari, "Control of systems integrating logic, dynamics, and constraints," *Automatica*, vol. 35, no. 3, pp. 407 – 427, 1999.
[23] J. Löfberg, "Automatic robust convex programming," *Optimization methods and software*, vol. 27, no. 1, pp. 115–129, 2012.